

Experimental testing and modeling the fluid loss and rheological behaviors of untreated and glass waste treated 6% bentonite water based drilling mud

Sahmee Eddwan Mohammed¹, Aram Mohammed Raheem^{2,}, Ibrahim Jalal Naser²*

¹ *College of Engineering, Petroleum Engineering Department, Kirkuk University, Kirkuk, Iraq*

² *College of Engineering, Civil Engineering Department, Kirkuk University, Kirkuk, Iraq*

Received November 7, 2024; Accepted March 24, 2025

Abstract

The main controlling characteristics of water based drilling mud are represented by infiltration and rheological properties. Hence, this study investigates the behavior of untreated and glass waste treated 6% bentonite water based drilling mud. The experimental work includes both infiltration tests at 100 psi (689 kPa) lasted for 30 minutes and rheological examinations at room temperature (25° C). The 6% bentonite water based drilling mud was treated with glass waste up to 50%. For both untreated and glass waste treated 6% bentonite water based drilling mud, the infiltration behavior was modeled using API and kinetic models while the rheological performance was predicted using four various models including Power Law, Bingham, Herschel-Buckley, and Hyperbolic models. The study has shown that for 30 minutes laboratory testing period, the tested 6% bentonite drilling mud had a maximum fluid loss of 13.6 cm³ whereas adding 20% glass to 6% bentonite drilling mud has increased the maximum fluid loss to 17.6 cm³. Moreover, adding 50% glass to 6% bentonite drilling mud has increased the maximum shear stress by 90% at 25° C testing temperature and this value was the greatest obtained shear stress compared to other tested glass treatments. Furthermore, all the utilized models for predicting the maximum shear stress for both untreated and glass treated 6% bentonite drilling mud were very good and the hyperbolic model was the best with a maximum R² of 0.9950 and a minimum RMSE of 0.2365 Pa.

Keywords: *Bentonite; Glass waste; Infiltration; Rheological properties; Kinetic model; Hyperbolic model.*

1. Introduction

Drilling fluids, often known as drilling muds, are a crucial element in the rotary drilling technique employed for oil and gas exploration both onshore and offshore. Drilling fluids, also known as muds, are a combination of chemicals, water, clay, and weighing material. They are utilized to remove cuttings from the drill bit and transport them to the surface [1-2]. The drilling mud comprises condensed liquids, which can be synthetic, oil-based, or water-based. The drill mud or fluid used in the drilling network is the sole component of the well-construction process that maintains an interface with the wellbore during the whole digging process. The drilling-fluid components are engineered to withstand extreme, wellbore conditions [3]. It contains a range of dense minerals and chemical additives. These substances are pumped through the drilling pipe to carry out certain duties [4]. Drilling muds serve several tasks, such as lubricating the drill bit, counterbalancing formation pressure, cleaning and conditioning the hole, maintaining hydrostatic pressure in the well, removing drill cuttings, and stabilizing the wall of the drilling hole [5]. Drilling fluids or mud gets depleted once they have served their purpose in the drilling procedures, therefore transforming them into waste products. Despite claims of being treated before disposal, these wastes are nevertheless considered a significant threat to both the environment and public health. This has prompted the need for detailed information regarding the detrimental effects of drilling fluids on public health. The analysis of the

constituents of used drilling mud, generated water, and drill cuttings, as well as the consequences of their disposal, mostly into aquatic ecosystems, in an effort by oil firms to comply with waste disposal environmental regulations, has received limited attention [6].

Water-based drilling cuttings (WDC) are the primary byproducts produced during the process of drilling and extracting shale gas [7]. While WDCs may not be classified as hazardous wastes in China, they nonetheless warrant significant concern due to their substantial quantities and potential for environmental degradation if not disposed of properly [8]. Typically, a solitary shale gas well in the southern Sichuan Basin would produce around 1500-2000 tons of wastewater discharge (WDC). As to the shale gas development plan of China National Petroleum Corporation, the region with a dense population and convoluted network of waterways may potentially accumulate from 4.5×10^5 to 7.8×10^5 tons of WDC year over the next 15 years. The proper disposal of WDC (waste drilling cuttings) has emerged as a constraining issue for the sustainable growth of shale gas [9-10].

Depending on their composition and intended applications, drilling fluids can be classified into many categories [11]. The selection of drilling fluid is influenced by three primary considerations: cost, practical application, and environmental impact. The presence of contaminants in drilling mud is a significant and potentially severe issue that can occur during drilling operations [12-13]. Mud is susceptible to contamination when any extraneous substance enters the mud system and causes undesirable alterations in the mud's characteristics, such as filtration, viscosity, and density. Water-based mud methods are particularly susceptible to contamination compared to other types of drilling mud. Mud pollution can arise from the excessive use of compounds in the mud network or from introducing foreign material during drilling. The primary pollutants in water-based drilling mud systems are solid gypsum/anhydrite, soluble sulfides, makeup water, salt/saltwater flow, cement/lime, and soluble carbonates and bicarbonates. Waste glass is a substantial constituent of municipal solid waste that must not be disregarded. Nevertheless, its non-biodegradable characteristics have presented a considerable environmental concern [14].

The rheological qualities mainly impacted including yield stress, plastic viscosity, filter cake, and gel strength. Protection against contamination and stability under various operating circumstances are also affected [15]. Several variables can influence the rheological characteristics of the drilling mud, including temperature, pressure, and pollutants [16-17]. The effectiveness and efficacy of drilling fluid in drilling operations are affected by its rheological characteristics. Therefore, it is necessary to examine the rheological characteristics and parameters of the drilling mud within downhole circumstances [18]. The glass addition to field soil has been added with different percentages and up to 20% to determine the impact on various rheological characteristics [19]. It was shown that the apparent viscosity for 20% glass-treated soil has been increased by 140% compared to untreated soil. The effect of temperature on the rheological properties of water based-drilling mud has been investigated [20]. It was shown that the maximum shear stress has been decreased by 42% as the temperature has been increased by three times (25°C to 75°C) for untreated drilling mud.

2. Objectives

The primary purpose of this work is concentrated on investigating the behavior of untreated and glass waste treated 6% bentonite water based drilling mud. The detailed objectives are focused on performing experimental testing for both infiltration and rheological characteristics for untreated and up to 50% glass waste treated 6% bentonite water based drilling mud. In addition, the infiltration behavior for untreated and glass waste treated 6% bentonite water based drilling mud was modeled using both API and kinetic models. On the other hand, the rheological performance for untreated and glass waste treated 6% bentonite water based drilling mud was predicted using four various models including Power Law, Bingham, Herschel-Buckley, and Hyperbolic models. Finally, the accuracy of all used models for both infiltration and rheology has been verified using coefficient of determination (R^2) and root mean square error (RMSE).

3. Methods

3.1. OFITE model 900 viscometer

The OFITE model 900 viscometer is a neat and portable device that is completely automated and designed for the precise measurement of fluid viscosity. The apparatus consists of a cylindrical rotating viscometer that employs a transducer to compute the angle of rotation caused by a fluid sample on the bob. The fluid being tested is retained within the shear gap or annular space between the rotor and bob, which is linked to a shaft equipped with a spring.

The fluid's viscous drag generates a torque on the bob, which is identified by the transducer to quantify the bob's angular displacement.

3.2. Filter press

The series 300 LPLT filter press, also known as the API Filter Press, is the main method used to evaluate the filtration characteristics of drilling muds and cement slurries. LPLT filter press assemblies consist of a frame that holds a mud reservoir, a pressure source, a filtering medium, and a regulated cylinder for collecting the filtrate. Based on the American Petroleum Institute (API), the designated working pressure is 100 psi (689 kPa), and the specified filtering area is 7.1 in² (46 cm²). The filter press design contains a cell body that includes the mud sample, a pressure intake, and a base cap equipped with a screen and filter press. The industry has utilized these units for both field and laboratory applications.

3.3. Drilling mud mixer

Drilling fluid formulations are typically blended utilizing various shearing devices that have either set or regulating speeds. The API suggests using a single mud impeller blade, which can take on several forms, such as rounded propellers, waveform shapes, and sharp blades. Additionally, these mixers can combine cement for laboratory or field-testing purposes.

4. Materials

4.1. Bentonite

The used bentonite is considered as a montmorillonite clay soil that is utilized as a main component in the drilling fluids to provide the necessary rheological characteristics. In addition, the main constituent for the water based mud is the bentonite as it determines the main functions represented by enhancing the viscosity and controlling the required filtration. The chemical interaction between bentonite and water results in bentonite swelling with water absorption. Bentonite as one of the natural absorbent clays and when such clay is interacted with water, bentonite with negative face is attracted by positive charge surfaces of water due to electrostatic attraction potentials. Due to the incident, the bentonite absorbs 7 to 10 times its weight and swell by 18 time its natural volume. There is a chemical reaction between several organic substances with bentonite and it develops mixtures that are utilized as gelling agents. Carrying the drilling cuts for circulation purposes is mainly dependent on the mud gel strength. The main used drilling mud is sodium bentonite, which is a high dispersive substantial with a high swelling potential. Another type of drilling mud is the calcium bentonite, which is not suitable to be utilized as a drilling mud because of its insignificant swelling potential that influences the mud rheology severely. Figure 1 shows a picture for the used bentonite.

4.2. Glass waste

The glass waste material is referred to the used old glass such as bottles, windows, and other glass-made products. Such waste products can be the outputs of households, businesses and industries. Glass waste material is durable that may need thousands of years to decay naturally. Thus, the management of glass waste is vital for environmental sustainability. The collected waste glass before and after grinding is shown in Figure 2.



Figure 1. A picture for the used bentonite.



Figure 2. Used glass waste material.

5. Modeling

5.1. Rheological characteristics

5.1.1. Power law

The power law model is a mathematical model used to describe a type of fluid known as a non-Newtonian fluid. In this model, there is an exponential association correlating the shear stress with the shear strain rate, which may be expressed as:

$$\tau = A_1 \gamma^{B_1} \quad (1)$$

where: τ and γ are the shear stress and shear strain rate, respectively; A_1 and B_1 are the fluid consistency unit and power law exponent, correspondingly.

$$\frac{d\tau}{d\gamma} = A_1 B_1 \gamma^{B_1-1} \quad (2)$$

$$\frac{d^2\tau}{d\gamma^2} = (B_1 - 1) A_1 B_1 \gamma^{B_1-2} \quad (3)$$

$$\text{As } \gamma = \infty \Rightarrow \tau_{\max} = \infty \quad (4)$$

Therefore, the criterion for the top limit of shear stress is not met when the power law is applied.

5.1.2. Bingham model

The Bingham model is a commonly used rheological model with two parameters that accurately describes the flow behavior of various drilling muds. The model can be written mathematically in the following form:

$$\tau = A_2 + B_2 \gamma \quad (5)$$

where: τ = the shear stress; γ = shear strain rate; A_2 is the yield point and B_2 is the plastic viscosity.

The fluid adheres to the Bingham model and reveals a linear association between shear stress and shear strain rate. The plastic viscosity (B_2) precisely indicates the gradient of the line, whereas the yield point (A_2) provides the minimum shear stress required to retain flow. The objective is to maintain a low B_2 level during fast drilling in order to reduce the presence of colloidal particles. The size of A_2 should be sufficient to facilitate the removal of cuttings from the hole while also avoiding excessive pump pressure during the initiation of mudflow. A_2 can be regulated by employing several methods of mud treatment.

5.1.3. Herschel-Bulkley model (H-B model)

The Herschel–Bulkley model defines a fluid using three parameters, which can be expressed mathematically as follows:

$$\tau = A_3 + B_3\gamma^{C_1} \quad (6)$$

where: τ and γ are the shear stress and shear strain rate, respectively; A_3 , B_3 , and C_1 are the yield stress, correction parameter, and flow behavior index, correspondingly.

The model proposes that, for the hard material, the slurry acts as a solid with no deformation below the yield stress (A_3), comparable to the Bingham plastic model. The exponent C_1 characterizes the shear thinning and shear thickening behavior of material flows that follow a Power law fluid model. Slurries are classified as exhibiting shear thinning behavior when the value of C_1 is less than 1 and shear thickening behavior when the value of C_1 is greater than 1. Shear thinning occurs when the apparent viscosity of a fluid lowers as the shear strain rate increases.

Therefore, the model must meet the following criteria:

$$\frac{d\tau}{d\gamma} = B_3C_1\gamma^{(C_1-1)} > 0 \Rightarrow B_3C_1 > 0 \quad (7)$$

$$\frac{d^2\tau}{d\gamma^2} = B_3C_1(C_1 - 1)\gamma^{(C_1-2)} > 0 \Rightarrow B_3C_1(C_1 - 1) < 0 \quad (8)$$

$$\text{As } \gamma = \infty \Rightarrow \tau_{\max} = \infty \quad (9)$$

Therefore, the Herschel-Bulkley model fails to meet the criterion for the maximum shear stress limit.

5.1.4. Hyperbolic model

A study was conducted to examine the association of the shear stress with the shear strain rate of water-based drilling mud. Depending on the evaluation of the laboratory test data, we can propose the existence of a hyperbolic relationship.

$$\tau - A_4 = \frac{B_4}{B_4 + D_1\gamma} \quad (10)$$

where: τ is the shear stress; and γ is the shear strain rate; A_4 is the yield stress while B_4 ; and D_1 are model parameters.

$$\frac{d\tau}{d\gamma} = \frac{(B_4 + D_1\gamma) \cdot (0) - B_4 \cdot D_1}{(B_4 + D_1\gamma)^2} = \frac{-B_4 \cdot D_1}{(B_4 + D_1\gamma)^2} > 0 \Rightarrow D_1 > 0 \quad (11)$$

$$\frac{d^2\tau}{d\gamma^2} = \frac{(B_4 + D_1\gamma)^2 \cdot (0) - B_4 \cdot D_1 \cdot 2 \cdot (B_4 + D_1\gamma) \cdot D_1}{(B_4 + D_1\gamma)^4} = \frac{-2B_4D_1^2}{(B_4 + D_1\gamma)^3} < 0 \Rightarrow D_1 > 0 \quad (12)$$

$$\text{As } \gamma \Rightarrow \infty \Rightarrow \tau_{\max} = \frac{1}{D_1} + A_4 \quad (13)$$

Evidently, this model demonstrates a constraint on the highest level of shear stress that the fluid can generate under significant shear strains.

5.2. Modeling of the filtering process

5.2.1. General model

The conventional approach for calculating the infiltration through a filter cake is determined using the following equations. The filter press is utilized to ascertain two factors: (1) the filtration rate on a standard filter paper and (2) the rate at which the thickness of the mud cake increases on the standard filter paper. According to Darcy's law, the infiltration rate can be expressed as:

$$\frac{dV_f}{dt} = \frac{k(t)A_o\Delta P}{\mu(T)h_{mc}} > 0 \quad (14)$$

During the filtration process, the amount of solid particles that enter the mud is equal to the amount of solid particles that accumulate in the filter cake.

$$f_{sm}(t)V_m = f_{sc}(t)h_{mc}A_o \quad (15)$$

where f_{sm} is the solid volume fraction in the mud and f_{sc} is the solid volume fraction in the formed cake.

$$f_{sm}(t)(h_{mc}A_o + V_f) = f_{sc}(t)(h_{mc}A_o) \quad (16)$$

$$h_{mc} = \frac{f_{sm}(t)V_f}{A_o(f_{sc}(t)-f_{sm}(t))} = \frac{V_f}{A_o\left(\frac{f_{sc}(t)}{f_{sm}(t)}-1\right)} \quad (17)$$

Substituting Eq. 17 into Eq. 14:

$$\int_0^{V_f} V_f dV_f = \int_0^t \frac{k(t)A_o\Delta P}{\mu(T)} A_o \left(\frac{f_{sc}(t)}{f_{sm}(t)} - 1 \right) dt \quad (18)$$

5.2.2. Static model (API model)

The static model has been constructed using the following assumptions:

1. The assumption that the filter cake is created initially needs to be corrected, as there is no cake creation at the beginning in both experimental and real field situations.
 2. The ratio of solids in the cake to the solids in the mud remains constant, but it actually increases over time until it reaches a maximum value when the flow ceases.
 3. The cake's permeability remains constant, yet, in actuality, it should diminish over time.
- By utilizing these assumptions and applying them to equation (15), and subsequently integrating with the given initial condition, the resulting equation is as follows:

$$V_f - V_o = \sqrt{2k\Delta P \left(\frac{f_{sc}}{f_{sm}} - 1 \right) A_o} \frac{\sqrt{t}}{\sqrt{\mu}} \quad (19)$$

Equation (19) is re-written as follows:

$$V_f - V_o = M * \sqrt{t} \quad (20)$$

where: V_o and V_f are the volumes of initial and final fluid loss (cm^3); respectively. k_o and k are initial and final permeability of drilling mud (Darcy); ΔP is the applied pressure (atm); f_{sc} and f_{sm} are the volume fractions of solids in the cake and mud, correspondingly. V_m is the solid volume in the mud (cm^3); A_o filter area (cm^2); t is the time (minute); μ is the mud viscosity (cp), h_{cm} is the filter cake thickness (cm).

$$M = \sqrt{2k\Delta P \left(\frac{f_{sc}}{f_{sm}} - 1 \right) A_o}$$

If the duration is assumed to be infinite (∞) in Equation (20), the volume of fluid loss will also be infinite (∞), which is not possible in reality. Therefore, the static (API) model does not meet the requirements for the total filtering volume.

5.2.3. New kinetic (hyperbolic) model

This model is formulated on the assumption that the rate of permeation is contingent upon many elements, including the permeability of the filter cake, the ratio of solid content in the cake to the solid content in the mud, and the duration of time.

$$\frac{dV}{dt} = f \left(k(t), \frac{f_{sc}}{f_{sm}}(t) \right) = Nk^L \left(\frac{f_{sc}}{f_{sm}} \right)^D \quad (21)$$

This model possesses the subsequent characteristics:

1. The quantification of the rate of change in permeability may be expressed using Equation 22, where L is equal to 1:

$$k = \frac{2A_5 * k_o}{(A_5 + B_5 t)^2} \quad (22)$$

2. The volumetric ratio of solid content in the cake to the solid content in the mud, as a function of time, is represented by Equation 23 with the parameter p set to 1:

$$\left(\frac{f_{sc}}{f_{sm}} - 1 \right) = \frac{\alpha_o t}{A_5 + B_5 t} \quad (23)$$

3. After substituting equations (22) and (23) into equation (18) and integrating the equation while applying the initial conditions, the filtration equation takes on the form of a hyperbolic function:

$$V_F - V_0 = N * \frac{t}{A_5 + B_5 t} \quad (24)$$

where: A_5 is the fluid loss parameter; B_5 is an arbitrary constant (1/min); α_o is an arbitrary constant (1/min); A_o is the filter area (cm²); V_o is the initial value of drilling mud infiltration (cm³); and $N = \sqrt{\frac{2k_o\alpha_o\Delta P}{\mu(T)}} A_o$.

The parameter A_5 indicates the rate at the beginning of the infiltration process, while the constant B_5 reflects the rate at the end of the infiltration process. In addition, Equation (24) fulfills the following criteria:

1. The total infiltration volume reaches a maximum value where further infiltration is prevented because a particle is obstructing all the available pores in the filter cake medium.
2. The API model does not allow for checking any of the specified qualities. However, these changes in the properties can be observed in the field or the laboratory. Furthermore, this model may be utilized to simulate infiltration-time relationships for both short and long durations.
3. Both A_5 and B_5 are dependent on both pressure and time.

6. Results and analysis

6.1. Preface

The findings and analysis of 12 laboratory experimental tests were conducted on water-based drilling mud. Six experiments were undertaken to simulate the filtration phenomena, while the other six experiments focused on measuring the rheological characteristics. The fluid loss studies were conducted at a pressure of 100 psi (689 kPa) on 6% untreated bentonite drilling mud. The duration of each test was 30 minutes. Experimental experiments were conducted on 6% bentonite drilling mud, treated with varying percentages of glass (ranging from 10% to 50% of the weight of bentonite). The tests were carried out at a pressure of 100 psi (689 kPa) and lasted for 30 minutes. The rheological studies were conducted on 6% untreated bentonite drilling mud at a constant temperature of 25°C. Experiments have been conducted on 6% bentonite drilling mud treated with varying percentages of glass (10% to 50% of the weight of bentonite) at a single temperature of 25°C. These experiments focused on the rheological properties of the mud.

6.2. Filtration experimental tests

Both the kinetic hyperbolic and API models were evaluated for their accuracy in predicting short-term results ($t = 30$ min). Although most laboratory or field tests may be conducted for more than 30 minutes, a 30-minute filtration phenomenon was done to confirm the typical API filtration laboratory test.

The graph in Figure 3 demonstrates the relationship between fluid loss and time for untreated 6% bentonite drilling mud at an applied pressure of 100 psi (689 kPa). The experimental test was conducted at ambient temperature and had duration of 30 minutes. Over time, the API model predicted exhibited unrestricted growth in fluid loss, in contrast to the kinetic hyperbolic model, which imposed a maximum restriction of $(V_o + N/B_5)$ on fluid loss. According to the experimental test, the 6% bentonite drilling mud had a maximum fluid loss of 13.6 cm³ after being tested for 30 minutes. The maximum fluid loss occurred when the mud was subjected to an applied pressure of 100 psi (689 kPa). The experimental data has been accurately predicted by both the API and Kinetic models, demonstrating excellent agreement.

Figure 4 illustrates the relationship between fluid loss and time for 6% bentonite drilling mud treated with 10% glass under an applied pressure of 100 psi (689 kPa). The experimental test was conducted at ambient temperature and had duration of 30 minutes. Based on the experimental test, it was found that the 6% bentonite drilling mud mixed with 10% glass had a maximum fluid loss of 13.2 cm³ after being tested for 30 minutes at an applied pressure of

100 psi (689 kPa). At an applied pressure of 100 psi (689 kPa), the maximum fluid loss increases by 3% as the glass treatment increases from 0% to 10%. The API and Kinetic models have accurately predicted the experimental results with a high level of agreement.

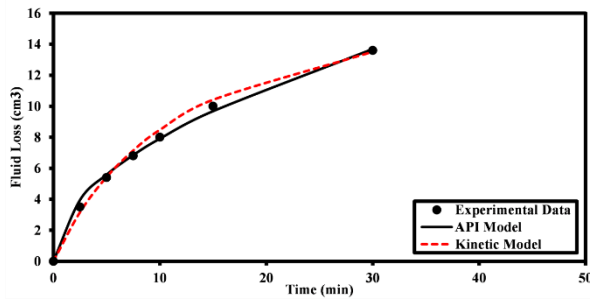


Figure 3. The variation of fluid loss versus time for untreated 6% bentonite drilling mud tested at room temperature under 100 psi (689 kPa).

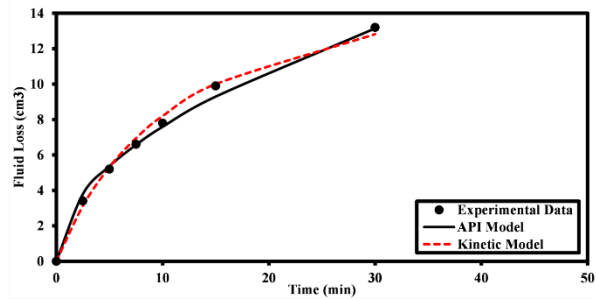


Figure 4. The variation of fluid loss versus time for 10% glass treated 6% bentonite drilling mud tested at room temperature under 100 psi (689 kPa).

The graphs in Figures 5, 6, 7, and 8 illustrate the changes in fluid loss over time for 6% bentonite drilling mud treated with 20%, 30%, 40%, and 50% glass, respectively, at an applied pressure of 100 psi (689 kPa). Experimental testing was conducted at ambient temperature and lasted for 30 minutes. The experimental tests have demonstrated that the 6% bentonite drilling mud, when treated with 20%, 30%, 40%, and 50% glass, experienced maximum fluid loss values of 17.6 cm³, 15.2 cm³, 13.2 cm³, and 16 cm³, respectively, after a final testing duration of 30 minutes. These results were obtained under an applied pressure of 100 psi (689 kPa). At an applied pressure of 100 psi (689 kPa), the maximum fluid loss increases by 29% for the glass increase from 0% to 20%.

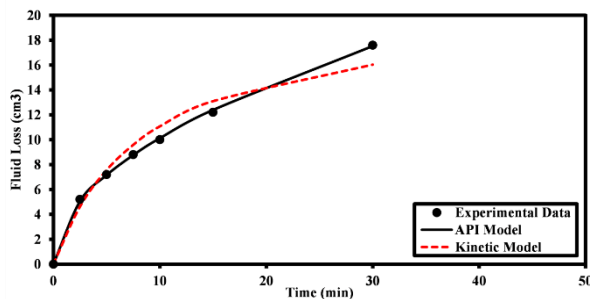


Figure 5. The variation of fluid loss versus time for 20% glass treated 6% bentonite drilling mud tested at room temperature under 100 psi (689 kPa).

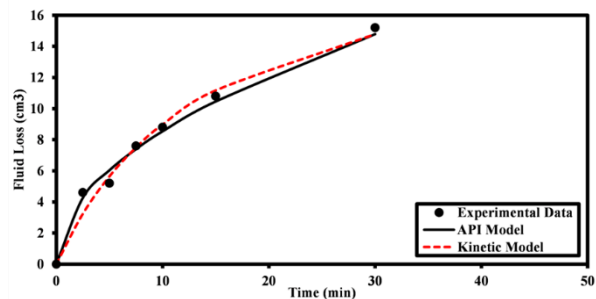


Figure 6. The variation of fluid loss versus time for 30% glass treated 6% bentonite drilling mud tested at room temperature under 100 psi (689 kPa).

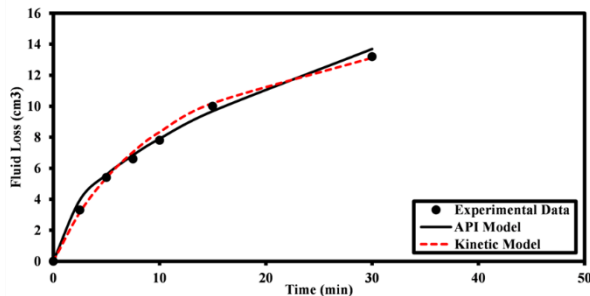


Figure 7. The variation of fluid loss versus time for 40% glass treated 6% bentonite drilling mud tested at room temperature under 100 psi (689 kPa).

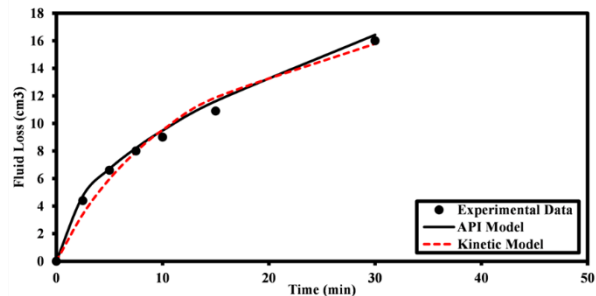


Figure 8. The variation of fluid loss versus time for 50% glass treated 6% bentonite drilling mud tested at room temperature under 100 psi (689 kPa).

The maximum fluid loss is fluctuated with different glass treatment, particularly; the final maximum fluid is increased by 29%, 12%, and 18% at 20%, 30% and 50% of glass treatment respectively. However, the final maximum fluid is decreased by 3% at 40% glass treatment.

Thus, 10% and 40% of glass treatments have the same effects in decreasing the maximum fluid loss by 3% while 20%, 30% and 50% of glass treatments have various impacts in increasing the final fluid loss. In general, the glass treatment has the tendency to increase the fluid loss due to their effect in separating the clay particles and facilitate the water to move faster in the same observed time.

The API and kinetic models have accurately forecasted the relationship between fluid loss and time for both untreated and glass-treated drilling muds. Table 1 presents a clear overview of the information pertaining to all the instances that were examined. Due to the mathematical fact that the API model represents an infinite fluid loss at an infinite time (which is impossible), the API model, along with the kinetic model, was able to correctly estimate the behavior of fluid loss throughout the analyzed period of 30 minutes. The API and Kinetic models achieved maximum R² values of 0.9995 and 0.9953, respectively. The minimal RMSE values for the API and Kinetic models were 0.1069 and 0.2725, respectively.

Table 1. Fluid loss model prediction parameters for untreated and glass treated bentonite drilling mud tested at 25°C.

Bentonite (%)	Glass (%)	API model				Kinetic model					
		V ₀ (cm ³)	M	R ²	RMSE(cm ³)	V ₀ (cm ³)	N	A ₅	B ₅	R ²	RMSE(cm ³)
6	0	0	2.5	0.9969	0.2273	0	0.5	0.33	0.026	0.9945	0.3018
6	10	0	2.4	0.9946	0.2912	0	0.5	0.33	0.028	0.9953	0.2725
6	20	0	3.2	0.9995	0.1069	0	0.31	0.13	0.015	0.9700	0.8852
6	30	0	2.7	0.9914	0.4155	0	0.35	0.23	0.016	0.9813	0.5846
6	40	0	2.5	0.9921	0.3542	0	0.35	0.23	0.019	0.9951	0.2801
6	50	0	3	0.9926	0.3993	0	0.4	0.25	0.017	0.9826	0.6145

To check the effectiveness of using the glass as a replacement material in the drilling mud, the maximum absolute fluid loss (%) was quantified as follows:

$$\text{Maximum Absolute Fluid Loss (\%)} = \frac{|A_6 - B_6|}{B_6} * 100 \quad (22)$$

where: A₆ is the maximum fluid loss value for glass treated drilling mud; and B₆ is the maximum fluid loss value for untreated drilling mud.

Figure 9 presents the value of the maximum absolute fluid loss (%) versus glass (%). The maximum absolute fluid loss (%) values of glass treated drilling mud were in the range of 3% to 29%. It should be noted that these values reveal that the glass trash can be used as a replacement material in the drilling mud with minimal effects on the fluid loss behavior. Accordingly, the glass material can be used as sustainable material in terms of preserving the fluid loss values within the acceptable limits.

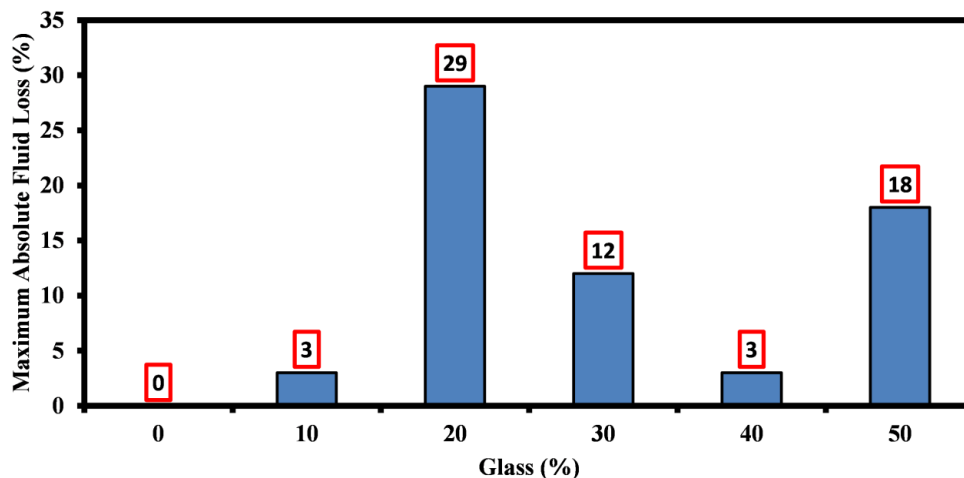


Figure 5. The variation of maximum absolute fluid loss (%) with glass (%).

6.3. Rheological characteristics analysis

A rheological experimental test was conducted on untreated 6% bentonite drilling mud at a temperature of 25°C. Furthermore, comparable experimental trials have been conducted on 6% bentonite drilling mud that was treated with different amounts of glass, ranging from 10% to 50% of the weight of bentonite.

The association of shear stress with the shear strain rate of untreated 6% bentonite drilling mud at a temperature of 25°C is illustrated in Figure 10. Four distinct models, including the power law, Bingham, Herschel-Buckley (H-B), and Hyperbolic models, have been employed. The accuracy forecasts for all the model parameters have been reported in Table 2. The untreated 6% bentonite drilling mud exhibited a maximum recorded shear stress of 18 Pa at a shear strain rate of 1021 (1/s) at a temperature of 25°C. The hyperbolic model outperformed all other models in predicting the maximum shear stress, with the greatest R² value of 0.9936 and the lowest RMSE value of 0.2826 Pa.

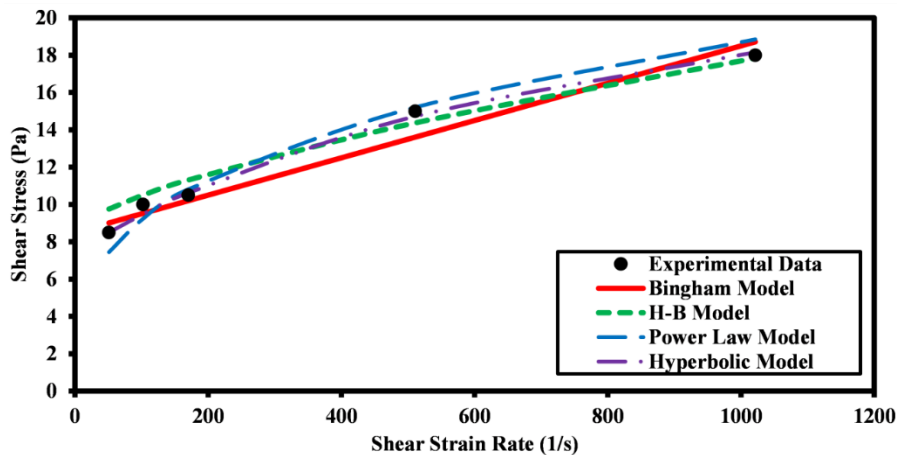


Figure 6. The variation of shear stress versus shear strain rate for untreated 6% bentonite drilling mud tested at 25°C.

Table 2. Models prediction parameters for untreated 6% bentonite drilling mud tested at 25°C.

Bentonite (%)	Glass (%)	Power law model					Bingham model				
		τ_0 (Pa)	A_1	B_1	R^2	RMSE(Pa)	A_2 (Pa)	B_2 (cP)	R^2	RMSE(Pa)	
6	0	7.45	2.2	0.31	0.9591	0.6533	8.5	0.01	0.9516	0.7782	
Bentonite (%)	Glass (%)	Herschel-Buckley (H-B) Model					Hyperbolic model				
		A_3 (Pa)	B_3 (Pa.s)	C_1	R^2	RMSE(Pa)	A_4 (Pa)	B_4 (cP)	D_1 (Pa ⁻¹)	R^2 (Pa ⁻¹)	RMSE(Pa)
6	0	8.5	0.09	0.67	0.9536	0.7619	8.5	50	0.052	0.9936	0.2826

The association of shear stress versus shear strain rate for a 10% glass (by weight of bentonite) treated with 6% bentonite drilling mud at a temperature of 25°C is illustrated in Figure 11. Four different models, namely the power law, Bingham, Herschel-Buckley (H-B), and Hyperbolic models, were utilized. The parameters of each model, along with their accuracy predictions, are summarized in Table 3. The maximum measured shear stress for the 10% glass-treated 6% bentonite drilling mud at 25°C was found to be 19.5 Pa at a shear strain rate of 1021 (1/s). All the models accurately predicted the maximum shear stress, with the hyperbolic model performing the best, exhibiting the highest R² value of 0.9860 and the lowest RMSE of 0.3178 Pa.

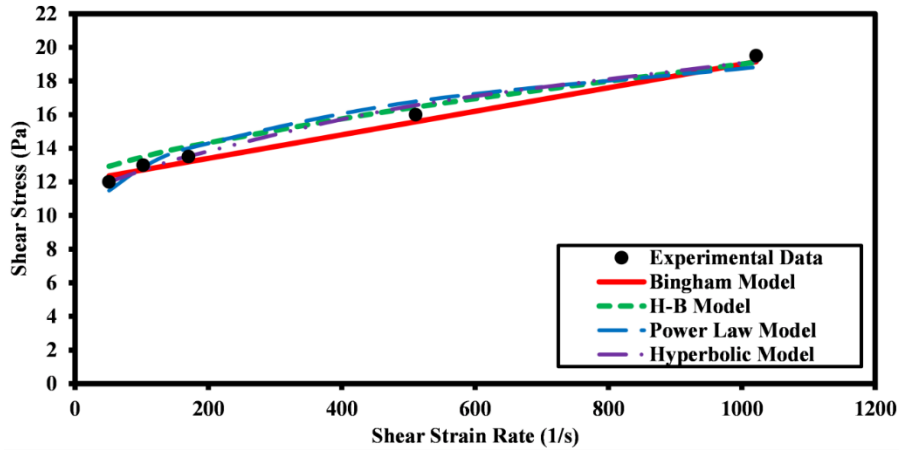


Figure 7. The variation of shear stress versus shear strain rate for 10% glass treated 6% bentonite drilling mud tested at 25°C.

Table 3. Models prediction parameters for 10% glass treated 6% bentonite drilling mud tested at 25°C.

Bentonite (%)	Glass (%)	Power law model					Bingham model				
		τ_0 (Pa)	A_1	B_1	R^2	RMSE(Pa)	A_2 (Pa)	B_2 (cP)	R^2	RMSE(Pa)	
6	10	11.48	6	0.165	0.9553	0.5196	12	0.007	0.9832	0.3486	
Bentonite (%)	Glass (%)	Herschel-Buckley (H-B) Model					Hyperbolic model				
		A_3 (Pa)	B_3 (Pa.s)	C_1	R^2	RMSE(Pa)	A_4 (Pa)	B_4 (cP)	D_1 (Pa ⁻¹)	R^2 (Pa) ⁻¹	RMSE(Pa)
6	10	12	0.064	0.68	0.9502	0.6012	12	70	0.067	0.9860	0.3178

The association of shear stress versus shear strain rate of a drilling mud containing 20% glass (by weight of bentonite) and 6% bentonite, treated at a temperature of 25°C, is depicted in Figure 12. Four distinct models, including the power law, Bingham, Herschel-Buckley (H-B), and Hyperbolic models, have been employed. The accuracy estimates for all the model parameters have been given in Table 4. The highest recorded shear stress for a drilling mud consisting of 20% glass and 6% bentonite at a temperature of 25°C was 28.5 Pa. The maximum shear stress occurred at a shear strain rate of 1021 (1/s). The hyperbolic model outperformed all other models in accurately predicting the maximum shear stress, with the greatest R^2 value of 0.9950 and the lowest RMSE value of 0.2365 Pa.

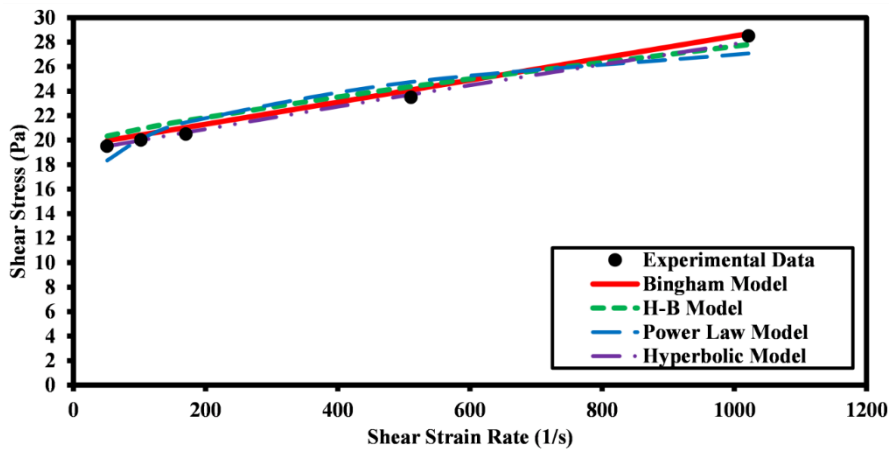


Figure 8. The variation of shear stress versus shear strain rate for 20% glass treated 6% bentonite drilling mud tested at 25°C.

Table 4. Models prediction parameters for 20% glass treated 6% bentonite drilling mud tested at 25°C.

Bentonite (%)	Glass (%)	Power law model					Bingham model				
		τ_0 (Pa)	A_1	B_1	R^2	RMSE(Pa)	A_2 (Pa)	B_2 (cP)	R^2	RMSE(Pa)	
6	20	18.34	11	0.13	0.8964	0.9846	19.5	0.009	0.9810	0.4610	
Bentonite (%)	Glass (%)	Herschel-Buckley (H-B) Model					Hyperbolic model				
		A_3 (Pa)	B_3 (Pa.s)	C_1	R^2	RMSE(Pa)	A_4 (Pa)	B_4 (cP)	D_1 (Pa ⁻¹)	R^2 (Pa) ⁻¹	RMSE(Pa)
6	20	19.5	0.04	0.77	0.9299	0.8875	19.5	105	0.009	0.9950	0.2365

The association of shear stress versus shear strain rate for a 30% glass (by weight of bentonite)-treated 6% bentonite drilling mud at a temperature of 25°C is identified in Figure 13. Four distinct models, including the power law, Bingham, Herschel-Buckley (H-B), and Hyperbolic models, have been employed. The accuracy forecasts for all the model parameters have been given in Table 5. The highest recorded shear stress for drilling mud containing 30% glass and 6% bentonite at a temperature of 25°C was 30.5 Pa. The maximum shear stress occurred at a shear strain rate of 1021 (1/s). The hyperbolic model outperformed all other models in predicting the maximum shear stress, with the greatest R^2 value of 0.9915 and the lowest RMSE value of 0.3249 Pa.

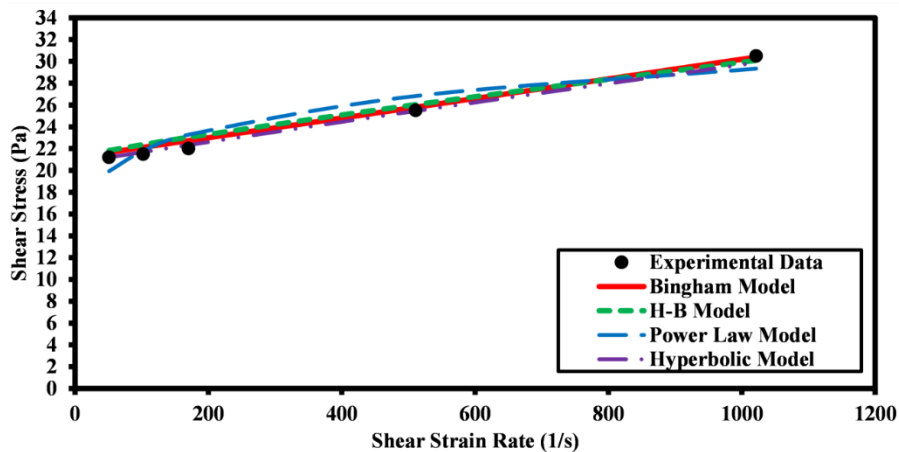


Figure 9. The variation of shear stress versus shear strain rate for 30% glass treated 6% bentonite drilling mud tested at 25°C.

Table 5. Models prediction parameters for 30% glass treated 6% bentonite drilling mud tested at 25°C.

Bentonite (%)	Glass (%)	Power law model					Bingham model				
		τ_0 (Pa)	A_1	B_1	R^2	RMSE(Pa)	A_2 (Pa)	B_2 (cP)	R^2	RMSE(Pa)	
6	30	19.93	12	0.129	0.8967	1.0368	21.2	0.009	0.9803	0.4959	
Bentonite (%)	Glass (%)	Herschel-Buckley (H-B) Model					Hyperbolic model				
		A_3 (Pa)	B_3 (Pa.s)	C_1	R^2	RMSE(Pa)	A_4 (Pa)	B_4 (cP)	D_1 (Pa ⁻¹)	R^2 (Pa) ⁻¹	RMSE(Pa)
6	30	21.2	0.02	0.88	0.9569	0.7339	21.2	105	0.007	0.9915	0.3249

The association of the shear stress versus shear strain rate of a 40% glass (by weight of bentonite)-treated 6% bentonite drilling mud at an ambient temperature of 25°C is presented in Figure 14. Four distinct models, including the power law, Bingham, Herschel-Buckley (H-B), and Hyperbolic models, have been employed. The accuracy forecasts for all the model parameters have been given in Table 6. The highest recorded shear stress for a drilling mud consisting of 40% glass and 6% bentonite, at a temperature of 25°C, was 33 Pa. The maximum shear stress occurred at a shear strain rate of 1021 (1/s). The hyperbolic model outperformed all other models in predicting the maximum shear stress, with the greatest R^2 value of 0.9949 and the lowest RMSE value of 0.3454 Pa.

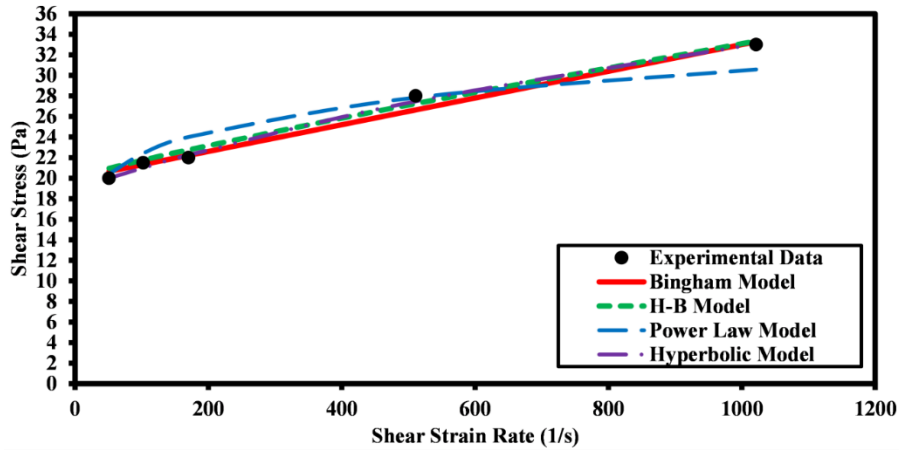


Figure 10. The variation of shear stress versus shear strain rate for 40% glass treated 6% bentonite drilling mud tested at 25°C.

Table 6. Models prediction parameters for 40% glass treated 6% bentonite drilling mud tested at 25°C.

Bentonite (%)	Glass (%)	Power law model					Bingham model				
		τ_0 (Pa)	A_1	B_1	R^2	RMSE(Pa)	A_2 (Pa)	B_2 (cP)	R^2	RMSE(Pa)	
6	40	20.40	12	0.135	0.9084	1.3486	20	0.013	0.9794	0.6993	
Bentonite (%)	Glass (%)	Herschel-Buckley (H-B) Model					Hyperbolic model				
		A_3 (Pa)	B_3 (Pa.s)	C_1	R^2	RMSE(Pa)	A_4 (Pa)	B_4 (cP)	D_1 (Pa ⁻¹)	R^2 (Pa ⁻¹)	RMSE(Pa)
6	40	20	0.03	0.88	0.9812	0.6683	20	50	0.025	0.9949	0.3454

The association of the shear stress versus shear strain rate of a drilling mud containing 50% glass (by weight of bentonite) and 6% bentonite at a temperature of 25°C is presented in Figure 15. Four distinct models, including the power law, Bingham, Herschel-Buckley (H-B), and Hyperbolic models, have been employed. The accuracy forecasts for all the model parameters have been given in Table 7. The highest recorded shear stress for a drilling mud consisting of 50% glass and 6% bentonite at a temperature of 25°C was 37 Pa. The maximum shear stress occurred at a shear strain rate of 1021 (1/s). All of the models accurately predicted the maximum shear stress. Among them, the Bingham model performed the best, with the greatest R^2 value of 0.9847 and the lowest RMSE value of 0.5338 Pa.

Table 7. Models prediction parameters for 50% glass treated 6% bentonite drilling mud tested at 25°C.

Bentonite (%)	Glass (%)	Power law model					Bingham model				
		τ_0 (Pa)	A_1	B_1	R^2	RMSE(Pa)	A_2 (Pa)	B_2 (cP)	R^2	RMSE(Pa)	
6	50	23.90	14	0.136	0.9429	0.9416	25	0.012	0.9847	0.5338	
Bentonite (%)	Glass (%)	Herschel-Buckley (H-B) Model					Hyperbolic model				
		A_3 (Pa)	B_3 (Pa.s)	C_1	R^2	RMSE(Pa)	A_4 (Pa)	B_4 (cP)	D_1 (Pa ⁻¹)	R^2 (Pa ⁻¹)	RMSE(Pa)
6	50	25	0.028	0.88	0.9766	0.6603	25	43	0.045	0.9834	0.5557

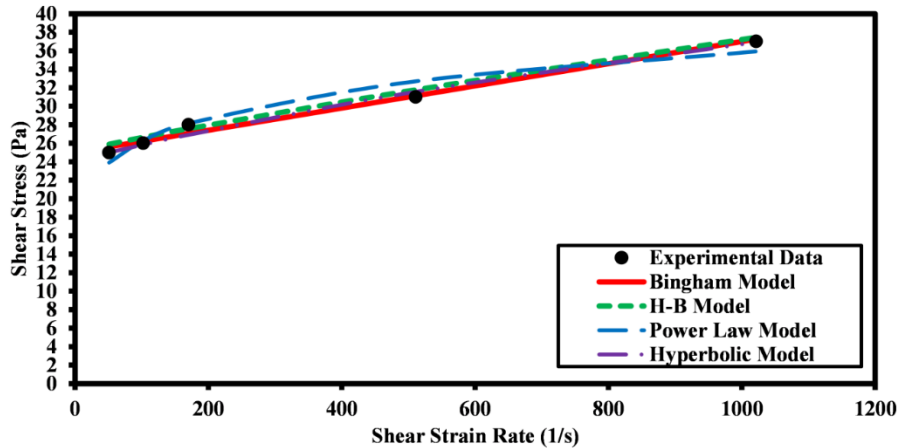


Figure 11. The variation of shear stress versus shear strain rate for 50% glass treated 6% bentonite drilling mud tested at 25°C.

7. Conclusion

The API fluid loss model has increased nonlinearly with time where this model has no limit for the maximum encountered fluid loss. However, the kinetic hyperbolic model limited the quantified maximum fluid loss by $(V_0 + N/B)$. Moreover, the kinetic model can take into account the effect of applied pressure whereas the API model ignored the effect of applied pressure. For 30 minutes laboratory testing period, the tested 6% bentonite drilling mud had a maximum fluid loss of 13.6 cm³ whereas adding 20% glass to 6% bentonite drilling mud has increased the maximum fluid loss to 17.6 cm³.

For the tested pressure of 100 psi (689 kPa) and at 30 minutes testing time, the maximum fluid loss is increased by 29% as the glass is increased from 0% to 20%. For 50% glass treatment, the maximum fluid loss of 6% bentonite drilling mud is increased by 18% for 100 psi (689 kPa) applied pressure and 30 minutes testing time. The maximum laboratory shear stress for 6% bentonite drilling mud was 18 Pa at 25° C testing temperature while adding 10% glass to 6% bentonite drilling mud has increased the maximum shear stress to 19.5 Pa for the same testing temperature.

Adding 50% glass to 6% bentonite drilling mud has increased the maximum shear stress by 90% at 25° C testing temperature and this value was the greatest obtained shear stress compared to other tested glass treatment. All the utilized models for predicting the maximum shear stress for both untreated and glass treated 6% bentonite drilling mud were very good and the hyperbolic model was the best with a maximum R² of 0.9950 and a minimum RMSE of 0.2365 Pa.

References

- [1] Antia M, Ezejiofor AN, Obasi CN, Orisakwe OE. Environmental and public health effects of spent drilling fluid: an updated systematic review. *Journal of Hazardous Materials Advances*, 2022; 7: 100120. <https://doi.org/10.1016/j.hazadv.2022.100120>
- [2] Fontes BLM, Souza LCSE, de Oliveira APSS, da Fonseca RN, Neto MPC, Pinheiro CR. The possible impacts of nano and microplastics on human health: lessons from experimental models across multiple organs. *Journal of toxicology and environmental health, Part B, Critical reviews* 27: 1-35. 2024; 18; 27(4):153-187. <https://doi.org/10.1080/10937404.2024.2330962>
- [3] Adewole G, Taiwo A, and Ufuoma E. Environmental aspect of oil and water-based drilling muds and cuttings from Dibi and Ewan off-shore wells in the Niger Delta, Nigeria. *African Journal of Environmental Science and Technology*, 2010;4(5): 284-292.
- [4] Al-Saleh I, Al-Sedairi A, and Elkhatib R. Effect of mercury (Hg) dental amalgam fillings on renal and oxidative stress biomarkers in children. *The Science of the total environment*, 2012; 431: 188-196. <https://doi.org/10.1016/j.scitotenv.2012.05.036>

- [5] Monitoring A. Assessment 2007: Oil and Gas Activities in the Arctic-Effects and Potential Effects. 2010; Volume 1. <http://hdl.handle.net/11374/704>
- [6] Liu W, Yuan H, Fan Z, Li J, Sun L. Using water-based drilling cuttings from shale gas development to manufacture sintered bricks: a case study in the southern Sichuan Basin, China. *Environmental Science and Pollution Research*, 2021; 28: 29379–29393. <https://doi.org/10.1007/s11356-021-12847-4>
- [7] Ayati B, Molineux C, Newport D, Cheeseman C. Manufacture and performance of lightweight aggregate from waste drill cuttings. *Journal of cleaner production*, 2019; 208: 252-260. <https://doi.org/10.1016/j.jclepro.2018.10.134>
- [8] Ball AS, Stewart RJ, and Schliephake K. A review of the current options for the treatment and safe disposal of drill cuttings. *Waste Management & Research*, 2012; 30(5): 457-473. <https://doi.org/10.1177/0734242X11419892>
- [9] Chen C, and Wu H. Lightweight bricks manufactured from ground soil, textile sludge, and coal ash. *Environmental Technology*, 2018; 39(11): 1359-1367. <https://doi.org/10.1080/09593330.2017.1329353>
- [10] Chen Y, Wu X, Yin W, Tang S, Yan G. Effects of Waste Glass Powder on Rheological and Mechanical Properties of Calcium Carbide Residue Alkali-Activated Composite Cementitious Materials System. *Materials*, 2023; 16(9): 3590. <https://doi.org/10.3390/ma16093590>
- [11] Raheem AM, and Vipulanandan C. Characterizing distinctive drilling mud properties using new proposed hyperbolic fluid loss model for high pressure and high temperature conditions. *Journal of King Saud University - Engineering Sciences*, 2022; 34(3): 217-229. <https://doi.org/10.1016/j.jksues.2020.10.002>
- [12] Ling T-C, and Poon C-S. Use of recycled CRT funnel glass as fine aggregate in dry-mixed concrete paving blocks. *Journal of cleaner production*, 2014; 68: 209-215. <https://doi.org/10.1016/j.jclepro.2013.12.084>
- [13] Raheem AM. "Study the Fluid Loss and Rheological Behaviors of Bentonite Drilling Mud Contaminated with Salt and Used Motor Oil. *Petroleum & Coal*, 2018; 60(6): 1087-1101.
- [14] Nasser J, Jesil A, Mohiuddin T, Al Ruqeshi M, Devi G, Mohataram S. Experimental investigation of drilling fluid performance as nanoparticles. *World Journal of Nano Science and Engineering*, 2013; 3(3): 27-61. <https://doi.org/10.4236/wjnse.2013.33008>
- [15] Azim RA. Evaluation of Production Potential of Fractured Geothermal Systems Due to Cold Fluid Circulation Under Poro-Thermo Elastic Conditions. *Petroleum and Coal*, 2017; 59(6): 975-990.
- [16] Amani M, Al-Jubouri M, and Shadravan A. Comparative study of using oil-based mud versus water-based mud in HPHT fields." *Advances in Petroleum Exploration and Development*, 2012; 4(2): 18-27. <https://doi.org/10.3968/j.aped.1925543820120402.987>
- [17] Zheng Y, She C, Yao K, Guo X, Zhang H, Yang T, Li M. Contamination effects of drilling fluid additives on cement slurry. *Natural Gas Industry B* 2(4): 354-359. <https://doi.org/10.1016/j.ngib.2015.09.009>
- [18] Nagre R, Zhao L, and Owusu P. Thermosaline Resistant Acrylamide-Based Polyelectrolyte as Filtration Control Additive in Aqueous-Based Mud. *Petroleum & Coal*, 2014; 56(3): 222-230.
- [19] Ali SQ, Raheem AM, Omar NQ, and Naser IJ. Glass waste impact on the rheological characteristics of field soil of Kirkuk city, Iraq. *IOP Conference Series: Earth and Environmental Science*, 1374(1): 012036. <https://doi.org/10.1088/1755-1315/1374/1/012036>
- [20] Raheem AM, and Vipulanandan C. Salt contamination and temperature impacts on the rheological and electrical resistivity behaviors of water based drilling mud. *Energy Sources, Part A: Recovery, Utilization, and Environmental Effects*, 2020; 42(3): 344-364. <https://doi.org/10.1080/15567036.2019.1587080>

To whom correspondence should be addressed: prof. Aram Mohammed Raheem, College of Engineering, Civil Engineering Department, Kirkuk University, Kirkuk, Iraq, E-mail: aram_raheem@uokirkuk.edu.iq; engaram@yahoo.com